Electronic to Vibrational Energy Transfer Assisted by Interacting Transition Dipole Moments: A Quantum Model for the Nonadiabatic $I_2(E) + CF_4$ Collisions

Yury V. Suleimanov and Alexei A. Buchachenko*

Laboratory of Molecular Structure and Quantum Mechanics, Department of Chemistry, Moscow State University, Moscow 119992, Russia

Received: May 7, 2007; In Final Form: July 2, 2007

We report a theoretical study of nonadiabatic transitions within the first-tier ion-pair states of molecular iodine induced by collisions with CF_4. We propose a model that treats the partner as a spherical particle with internal vibrational structure. Potential energy surfaces and nonadiabatic matrix elements for the I_2-CF_4 system are evaluated using the diatomics-in-molecule perturbation theory. A special form of the intermolecular perturbation theory for quasi-degenerate electronic states is implemented to evaluate the corrections to the long-range interaction of transition dipole moments of colliding molecules. The collision dynamics is studied by using an approximate quantum scattering approach that takes into account the coupling of electronic and vibrational degrees of freedom. Comparison with available experimental data on the rate constants and product state distributions demonstrates a good performance of the model. The interaction of the transition dipole moments is shown to induce very efficient excitation of the dipole-allowed υ_3 and υ_4 modes of the CF_4 partner. These transitions proceed predominantly through the near-resonant E−V energy transfer. The resonant character of the partner's excitation and the large mismatch in vibrational frequencies allow one to deduce the partner's vibrational product state distributions from the distributions measured for the molecule. The perspectives of the proposed theoretical model for treating a broad range of molecular collisions involving the spherical top partners are discussed.

I. Introduction

Studies of gas-phase energy transfer involving polyatomic molecules are still challenging for molecular collision theory. Collisions with the spherical top (ST) molecules (most commonly CH_4, CF_4, or SF_6) can be considered as a relatively simple case due to high symmetry facilitating approximate treatments.[1,2] ST molecules are known to be quite specific and efficient acceptors of energy in various quenching and relaxation processes. For instance, experimental studies of the $O_2(X)$ and $N_2(A)$ vibrational relaxation on some ST partners indicate the predominant role of the near-resonant V−V energy transfer;[3,4] time-of-flight measurements[5] and semiclassical modeling[1] evidence efficient vibrational excitation of the CH_4, CF_4, and SF_6 by atomic ions, and manifestation of the E−V contribution can be seen in the quenching of electronically excited atoms.[6] In some of these papers, speculations were made about the long-range (LR) near-resonant mechanism of the partner's vibrational excitation. However, this mechanism is difficult to elucidate without direct experimental probing or state-resolved theoretical calculations of the vibrational product state distributions (VPDs) of the partner.

It turns out that reasonable state resolution for the partner may be achieved without any experimental complication in collisions of heavy molecules whose vibrational quantum is much less than those of the partner. The VPDs measured for such molecules may reveal the structure associated with the partner's vibrational excitations. It is exactly the case analyzed by Pravilov et al. for collisions of iodine molecules excited to ion-pair (IP) state $E0_g^+$.[7,8] Measured vibrational distributions of the $I_2(D0_u^+)$ products formed in the collision-induced nonadiabatic transition (CINAT) on the CF_4 partner exhibit a well-resolved structure associated with υ_3 and υ_4 vibrational excitations. These results provide a unique opportunity for developing and testing theoretical models for energy-transfer processes involving ST partners.

It is important to emphasize that CINATs between IP states of molecular iodine are interesting by themselves. A number of studies devoted to the CINATs' dynamics of the ion-pair (IP) states of molecular iodine[7−18] (earlier bibliography can be found in refs 9 and 19) indicates that these processes provide a unique model for understanding the kinetics and mechanisms of electronic energy transfer in dense manifolds of vibronic states.[9]

In iodine, as well as in other halogen molecules, the IP states lie just above the valence electronic states and correlate to the ionized $I^+ + I^-$ dissociation limits.[20,21] According to the asymptotic energy determined by the electronic state of the I^+ cation, the IP states fall into several tiers of strongly bound potential energy curves with very similar, although not exactly equal, molecular constants. The first tier correlates to the $I^+(^3P_2) + I^-(^1S_0)$ limit and consists of the six states, $E0_g^+$, $D0_u^+$, $\beta 1_g$, $\gamma 1_u$, $D'2_g$, and $\delta 2_u$, classified within the Hund case (c) coupling scheme. Populating different vibronic levels and detecting the product fluorescence, one can gain an insight into the dependence of the nonadiabatic pathways on symmetry, wave function overlap, and energies of the levels involved. The straightforward access to the E state via the optical−optical double resonance (OODR) excitation and relatively short lifetimes of the IP states greatly facilitates the state-resolved experimental studies of the CINAT under the single-collision

* To whom correspondence should be addressed. Phone: +7 495 939 22 86. Fax: +7 495 939 24 13. E-mail: alexei@classic.chem.msu.su.

10.1021/jp073472+ CCC: $37.00
Published on Web 08/29/2007

conditions, although the overlapping spectral bands may complicate the fluorescence analysis.[9]

The IP states possess few important specific features. Their electronic structure can be described by a resonant charge separation model.[9,22] It implies that the IP states of the same spatial symmetry but opposite permutation parity u/g (like $E-D$, $\beta-\gamma$, and $D'-\delta$ pairs in the first tier) are connected by the giant transition dipole moments.[22,23] These moments can couple with the instantaneous, permanent, or transition electric moments of the collision partner, thus providing a strong dependence of the long-range intermolecular interactions on the nature of the partner. Pravilov and co-workers[7] followed by others[10,11] were the first to analyze the contributions of such long-range interactions to the nonadiabatic couplings.

Collisions with the rare gas atoms (Rg) represent the simplest case when only the instantaneous dipole moments contribute. The resulting induction-like correction to the interaction potential energy surfaces (PESs) was derived in refs 10 and 11. The $I_2(E)$ + Rg collisions were thoroughly analyzed both experimentally and theoretically.[9] The most refined theoretical approach[10,11,14] combines the diatomics-in-molecule[16,24] and long-range[10,11] perturbation theories for the diabatic PESs and couplings with an approximate quantum scattering method adapted to collisions of heavy molecules obeying the Hund case (c) coupling scheme.[9,25]

Nonadiabatic transitions induced by collisions with molecular partners were also investigated experimentally. The state-resolved OODR measurements were performed for collisions with $I_2(X0_g^+)$, N_2,[7,8,17] and CF_4[7,8,18] molecules. Their results qualitatively confirm the importance of long-range interactions between the IP transition moment and the moments of the partner and the significant role of the E−V energy transfer. VPDs observed for the CF_4 provide an especially clear picture of the partner's vibrational excitation.[7]

The aim of the present study is threefold. First, we develop a practical theoretical model for studying the quantum dynamics of the $I_2(E)$ + CF_4 collisions and test it against available experimental data. Second, we analyze the long-range interactions in this system and show that the coupling between the electronic and vibrational transition dipole moments of two molecules is responsible for efficient near-resonant E−V energy transfer. Manifestations of this mechanism are also discussed in relation to previous findings for the $I_2(E)$ + Rg collisions. Third, we consider overall performance of the model and its perspectives for the broader range of energy transfer processes involving spherical top partners.

II. Theoretical Model

1. Hamiltonians and Channel Functions. The total electron−nuclear Born−Oppenheimer Hamiltonian for the I_2 + A system, where A is a ST molecule, can be written as

$$\hat{H}_{tot} = -\frac{1}{2\mu R^2}\frac{\partial}{\partial R}R^2\frac{\partial}{\partial R} + \frac{\hat{l}^2}{2\mu R^2} + \hat{H}_{I_2} + \hat{H}_A + \hat{V} \quad (1)$$

where R is the center-of-mass separation of the colliding particles, l is the orbital angular momentum for the collision, μ is the reduced mass of the colliding particles, $\hat{V}$ is the interaction potential, and $\hat{H}_{I_2}$ and $\hat{H}_A$ denote the Hamiltonians of isolated I_2 and A molecules, respectively. The Hamiltonian of the I_2 molecule is

$$\hat{H}_{I_2} = -\frac{1}{2mr^2}\frac{\partial}{\partial r}r^2\frac{\partial}{\partial r} + \frac{\hat{j}^2}{2mr^2} + \hat{H}^{el}_{I_2}(r; q_{I_2}) \quad (2)$$

where r is the internuclear distance and m is the reduced mass, j corresponds to the total molecular angular momentum within the Hund case (c) coupling scheme, $\hat{H}^{el}_{I_2}$ is the electronic Hamiltonian, and q_{I_2} denotes collective coordinate of all electrons formally assigned to the I_2 molecule. The Hamiltonian of the molecule A is represented as

$$\hat{H}_A = \hat{T}(Q) + \hat{H}^{el}_A(Q; q_A) \quad (3)$$

where T is the nuclear kinetic energy operator, Q denotes the internal nuclear coordinates, and $\hat{H}^{el}_{I_2}$ is the electronic Hamiltonian that depends on q_A, the collective coordinate of all electrons assigned to A.

The asymptotic solutions of the Schrödinger equation with the Hamiltonian (eq 1) can be expressed in terms of the eigenfunctions of Hamiltonians (eqs 2 and 3)

$$\hat{H}_{I_2}|n\Omega\sigma w;v_n jm\rangle = E_{nv_n j}|n\Omega\sigma w;v_n jm\rangle$$
$$\hat{H}_A|f;v_A JMK\rangle = \epsilon_{fv_A J}|f;v_A JMK\rangle \quad (4)$$

and

$$E_{nv_n jfv_A J} = E_{nv_n j} + \epsilon_{fv_A J} \quad (5)$$

are the respective asymptotic channel energies. The eigenfunctions (eq 4) are represented as the products of electronic, rotational, and vibrational parts. For iodine

$$|n\Omega\sigma w;v_n jm\rangle = |n\Omega\sigma w\rangle|v_n\rangle|\,jm\Omega\rangle \quad (6)$$

where n is the electronic state label, Ω and m are the projections of j onto the molecule-fixed (MF) and space-fixed (SF) axes, respectively, σ is the parity with respect to reflection in the molecular plane, w specifies the permutation symmetry, and v_n is the vibrational quantum number. For A

$$|f;v_A JMK\rangle = |\,f\rangle|v_A\rangle|\,JMK\rangle \quad (7)$$

where f labels the electronic states, v_A and J are vibrational and rotational quantum numbers, and M and K specify the projections of J onto the SF and MF axes, respectively. In the frame of the scattering problem, we will consider only the ground electronic state of A ($f = 0$).

2. Quantum Scattering Equations. To solve the scattering problem, one needs to expand the total scattering wave function over the channel functions introduced above and insert it into the time-independent Schrödinger equation to obtain the system of close-coupled (CC) equations, which determines, asymptotically, the scattering amplitudes and S matrices for each partial wave l. Numerical solution of the resulting system is, however, extremely demanding due to the large number of coupled scattering channels. For much simpler collisions with the atomic Rg partner, it is possible only when an approximate treatment is invoked for the rotational degrees of freedom of I_2.[25] The most accurate method available in this case, the so-called EVCC-IOS approximation, uses the CC treatment of the electronic and vibrational degrees of freedom of the I_2 molecule and the infinite-order sudden (IOS) approximation for rotational motion.[25] We employed the same approximation here and, in addition, disregarded the rotational motion of the partner A, considering it as a spherical particle. Replacing $|JMK\rangle$ by $|000\rangle$, one eliminates the dependence of the interaction operator on the orientation of the partner with respect to the R axis and arrives at the same system of EVCC-IOS equations as before,[25]

with the only difference that the transitions between the vibrationally excited levels of the A molecule are included

$$\left[\frac{d^2}{dR^2} - \frac{\bar{l}\,(\bar{l}+1)}{R^2} + k^2_{n\nu_n \bar{j} v_A}\right] F^{\bar{l}\bar{j}}_{n\Omega\nu_n v_A}(R;\theta) = 2\mu \sum_{n'\Omega',\nu_{n'},v'_A} V_{n'\nu_{n'}v'_A,n\nu_n v_A} F^{\bar{l}\bar{j}}_{n'\Omega'\nu_{n'}v'_A}(R;\theta) \quad (8)$$

Here, $\bar{l}$ and $\bar{j}$ are the effective average values of the corresponding angular momentum operators which parametrize the IOS approximation,[26] θ is the angle between the R and r vectors, and $V_{n'\nu_n\nu'_A,n\nu_n\nu_A}$ are the matrix elements of the interaction operator

$$V_{n'\nu_{n'}v'_A,n\nu_n v_A}(R,\theta) = \langle \nu_{n'}|\langle v'_A\,|V_{n'n}(R, r, \theta, Q)|v_A\rangle|\nu_n\rangle \quad (9)$$

where

$$V_{n'n}(R, r, Q, \theta) = \langle n'\Omega'\sigma'w'|\langle f=0|\hat{V}(R, r, \theta, Q; q_{I_2}, q_A)|f=0\rangle|n\Omega\sigma w\rangle \quad (10)$$

The wave vector $k^2_{n\nu_n\bar{j}v_A} = 2\mu(E - E_{n\nu_n\bar{j}} - \epsilon_{0v_A0})$ depends on the total energy E and the channel energies given by eq 4.

The radial functions $F^{\bar{l}\bar{j}}_{n'\Omega'\nu_{n'}v_A}$ depend on the θ angle only parametrically through the anisotropy of the potential matrix elements. The system of eq 8 is solved at fixed θ values, and the scattering S matrix $S(\theta)$ is defined by the standard IOS boundary conditions applied to the radial solutions $F^{\bar{l}\bar{j}}_{n'\Omega'\nu_{n'}v_A}$ in the asymptotic region.[25,27] Expanding the S matrix elements over the reduced Wigner d functions

$$S^{\bar{l}\bar{j}}_{n'\Omega'\nu_{n'}v_A,n\Omega\nu_n v_A}(\theta) = \sum_\lambda S^{\bar{l}\bar{j}}_{n'\Omega'\nu_{n'}v_A,n\Omega\nu_n v_A;\lambda} d^\lambda_{0,\Omega'-\Omega}(\cos\theta) \quad (11)$$

and identifying $\bar{l}$ with the initial orbital momentum,[26] one defines the electronically inelastic cross sections $\sigma_{n'\Omega'\nu_{n'}j'v'_A,n0\nu_n j v_A}$ as

$$\sigma_{n'0\nu_n j'v'_A,n0\nu_n j v_A} = \frac{\pi(2j'+1)g_{v'_A}}{k^2_{n\Omega\nu_n\bar{j}v_A} g_{v_A}} \sum_\lambda \sum_l \frac{2l+1}{2\lambda+1} \left|\begin{pmatrix} j' & \lambda & j \\ 0 & 0 & 0\end{pmatrix} S^{\bar{l}\bar{j}}_{n'0\nu_n j'v'_A,n0\nu_n j v_A;\lambda}\right|^2 \quad (12)$$

if $\Omega' = 0$ and as

$$\sigma_{n'\Omega'\nu_n j'v'_A,n0\nu_n j v_A} = \frac{\pi(2j'+1)g_{v'_A}}{k^2_{n\Omega\nu_n\bar{j}v_A} g_{v_A}} \sum_\lambda \sum_l \frac{2l+1}{2\lambda+1} \times \left|\begin{pmatrix} j' & \lambda & j \\ -\Omega' & \Omega' & 0\end{pmatrix} [S^{\bar{l}\bar{j}}_{n'\Omega'\nu_{n'}v'_A,n0\nu_n v_A;\lambda} + \eta S^{\bar{l}\bar{j}}_{n'-\Omega'\nu_{n'}v'_A,n0\nu_n v_A;\lambda}]\right|^2 \quad (13)$$

if $\Omega' \neq 0$. Here, η can take the values of ± 1 according to the parity of the molecular functions (see ref 25), and the g_{v_A} factors account for the degeneracy of the vibrational state of the partner. These two equations hold for $\Omega = 0$, for example, for initial state $E0^+_g$. Rotationally summed cross sections are expressed as

$$\sigma_{n'\nu_{n'}v'_A,n\nu_n j v_A} = \sum_{j'} \sigma_{n'\Omega'\nu_n j'v'_A,n0\nu_n j v_A} \quad (14)$$

3. Diabatic PESs and Couplings for the $I_2(E)-CF_4$ System. The model used to approximate the matrix elements of the interaction potential operator (eq 9)—diabatic PESs and couplings—resembles that developed previously for the I_2-Rg systems.[9−11,16] It combines the first-order diatomics-in-molecule perturbation theory (DIM PT1)[24] with the perturbative treatment in the spirit of the so-called "diatomics-in-ionic-systems" model by Last and George,[28,29] formulated perturbatively (see, e.g., refs 30−32). The short-range DIM PT1 model treats the partner as an effective atom and is therefore the same as that for the I_2-Rg interactions.[9−11,16] In contrast, the treatment of the long-range interaction accounts for the specific features of the system under study.

Long-Range Interaction. Very strong dipole coupling between the IP states of the same symmetry and opposite permutation parity has been already mentioned.[7,10,22] To elucidate the effect of this feature on the long-range intermolecular interaction, we have developed a special form of the intermolecular perturbation theory.[10,15] Here, we apply it for interaction with the CF_4 molecule.

In terms of the spherical tensor operators, the lowest-order dipole−dipole interaction can be written as[33]

$$\hat{V}_{dd} = -8\left(\frac{2\pi^3}{3}\right)^{1/2} \frac{\hat{\mu}(r;q_{I_2})\hat{d}(Q;q_A)}{R^3} \sum_{m=-1}^{1} \begin{pmatrix} 1 & 1 & 2 \\ m & -m & 0\end{pmatrix} Y_{1m}(\hat{\Omega}_{I_2}) Y_{1-m}(\hat{\Omega}_A) Y_{20}(\hat{\Omega}) \quad (15)$$

where the angles $\hat{\Omega}_{I_2}$, $\hat{\Omega}_A$, and $\hat{\Omega}$ specify the orientation of the electronic distribution of the I_2 and CF_4 fragments with respect to their own quantization axes and the interfragment axis R, respectively, Y_{lm} are the spherical harmonics, and the dipole moment operators of I_2 and CF_4 are denoted as μ and d, respectively.

The matrix elements of the operator (eq 15) in the asymptotic channel basis $|n\Omega\sigma w\rangle|\nu_n\rangle|f=0\rangle|v_A\rangle$ contribute to the interaction potential matrix (eq 9). For simplicity, we first consider the integrals over the electronic and vibrational coordinates and then include the angular factors.

For the I_2 fragment, all of the diagonal elements vanish

$$\langle n\Omega\sigma w|\hat{\mu}(r;q_{I_2})|n\Omega\sigma w\rangle = \langle n|\hat{\mu}|n\rangle = 0 \quad (16)$$

while among the nondiagonal elements, we retained only those that connect strongly coupled states n, n' of the same symmetry and opposite permutation parities

$$\langle n|\hat{\mu}(r;q_{I_2})|k\rangle = \delta_{kn'}\mu_{nn'}(r) \quad \langle n'|\hat{\mu}(r;q_{I_2})|k\rangle = \delta_{kn}\mu_{nn'}(r) \quad (17)$$

For the CF_4 fragment in the ground electronic state $f=0$, all of the diagonal matrix elements also vanish

$$\langle v_A|\langle f=0|\hat{d}(Q;q_A)|f=0\rangle|v_A\rangle = 0 \quad (18)$$

Among the nondiagonal matrix elements, especially important (and the only ones known) are those associated with vibrational excitations from the initial ground level v_0

$$\langle v_0|\langle f=0|\hat{d}(Q;q_A)|f=0\rangle|v_i\rangle = d_{0i} \quad (19)$$

where $i = 3$ and 4 correspond to the CF_4 IR-active fundamentals v_3 and v_4; therefore, $d_{03} = 1.02$ D and $d_{04} = 0.14$ D are the dipole moments of the $[0,0,1,0]f_2 \leftarrow [0]$ (1283 cm^{-1}) and $[0,0,0,1]f_2 \leftarrow [0]$ (631.2 cm^{-1}) transitions, respectively.[34,35] Both excited states are triply degenerate; therefore, $g_{v_3} = g_{v_4} = 3$ and $g_{v_0} = 1$ in eqs 12 and 13.

The explicit expression for the dipole−dipole coupling matrix elements is

$$\langle v_0|V^{(1)}_{dd,nn'}|v_i\rangle = -\frac{\mu_{nn'}d_{0i}}{R^3}(2\cos\theta\cos\theta_A - \sin\theta\sin\theta_A\cos\varphi_A) \quad (20)$$

where the angles θ_A and φ_A specify the orientation of the d vector with respect to the R axis. These matrix elements cannot be defined within the approximate model of rotational motion of CF_4 used in this work, while the simple averaging over θ_A and φ_A completely eliminates the matrix element (eq 20). Holtermann et al.[36] suggested to "maximize" the dipole−dipole term by fixing θ_A at zero. We use a slightly different approach[7,37] and perform the averaging with the weighting factor $\cos\theta_A$. It gives

$$V^{LR,1}_{nn',v_0v_i}(r,R,\theta) = -\frac{2\mu_{nn'}(r)d_{0i}}{3R^3}\cos\theta \quad (21)$$

Equation 21 represents the LR limit of the diabatic coupling between the n and n' states connected by the large dipole moment.

The second-order LR correction can be approximated in exactly the same way as that reported before for the I_2−Rg systems.[10,11] In brief, we disregard the vibrational structure of the CF_4 partner but take into account electronic excitations to the $f \neq 0$ states. These states perturb the pair of IP states n, n' of I_2 through the dipole−dipole interaction. Using the van Vleck transformation (see, e.g., ref 38) one obtains

$$V^{(2)}_{dd,nn'} = 0 \quad V^{(2)}_{dd,nn} = V^{(2)}_{dd,n'n'} \propto \mu^2_{nn'}\sum_{f\neq 0}\frac{\langle 0|\hat{d}|f\rangle\langle f|\hat{d}|0\rangle}{E_n - E_{n'} + \epsilon_0 - \epsilon_f} \quad (22)$$

where E_n, $E_{n'}$ and ϵ_0, ϵ_f denote the electronic energies of the I_2 and CF_4 fragments, respectively. Taking into account that for close-lying IP states $|E_n - E_{n'}| \ll \epsilon_f - \epsilon_0$, one can estimate the sum in eq 22 through the static dipole polarizability of the CF_4 fragment

$$\sum_{f\neq 0}\frac{\langle 0|\hat{d}|f\rangle\langle f|\hat{d}|0\rangle}{E_n - E_{n'} + \epsilon_0 - \epsilon_f} \approx -\sum_{f\neq 0}\frac{\langle 0|\hat{d}|f\rangle\langle f|\hat{d}|0\rangle}{\epsilon_f - \epsilon_0} = -\frac{3}{2}\alpha_A$$

Evaluation of the angular part and averaging over the angles θ_A and φ_A give

$$V^{LR,2}_{nn}(r,R,\theta) = V^{LR,2}_{n'n'}(r,R,\theta) = -\frac{\mu^2_{nn'}(r)\alpha_A}{2R^6}(3\cos^2\theta + 1) \quad (23)$$

This equation defines the LR correction for the DIM PT1 interaction PESs. We used the value of $\alpha_A = 19.51$ au from ref 39.

The $\mu_{nn'}$ functions are not known exactly, but the resonant charge separation model, as well as the experimental data,[23] suggests a simple expression

$$\mu_{nn'}(r) = e\cdot r \quad (24)$$

where e is the unit charge.

First-Order Diatomics-in-Molecule Perturbation Theory. In the DIM PT1 method, the total electronic Born−Oppenheimer Hamiltonian is separated into the zero-order term

$$\hat{H}^0_{DIM} = \hat{H}^{el}_{I_2}(r;q_{I_2}) + \hat{H}^{el}_A(Q;q_A) \quad (25)$$

and perturbation

$$\hat{V}_{DIM}(R,r,Q;q_{I_2},q_A) = [\hat{H}^{el}_{A-I_a} - \hat{H}^{el}_{I_a} - \hat{H}^{el}_A] + [\hat{H}^{el}_{A-I_b} - \hat{H}^{el}_{I_b} - \hat{H}^{el}_A] \quad (26)$$

where a and b distinguish identical iodine centers. The electronic Hamiltonians in eq 25 were incorporated into the Hamiltonians of the isolated fragments (eqs 2 and 3); therefore, the perturbation term (eq 26) gives the interaction $\hat{V}$ in eq 1. The eigenfunctions of the zero-order electronic Hamiltonians (eq 25) are therefore the products of the $|n\Omega\sigma w\rangle$ and $|f\rangle$ functions introduced by eqs 6 and 7. In what follows, we will ignore the dependence of the $|f = 0\rangle$ function on the internal coordinates Q. The matrix elements of the $\hat{V}_{DIM}$ operator (eq 26) can be then evaluated in the same way as that for the I_2−Rg systems.

The corresponding procedure is well documented.[9,10,16] In brief, the $|n\Omega\sigma w\rangle$ functions are expanded, asymptotically, over the products of atomic electronic functions describing the iodine centers in the charged states $I^+(^3P_2)$ and $I^-(^1S_0)$. This expansion allows one to evaluate the $\langle n\Omega\sigma w;f = 0|\hat{V}_{DIM}|n'\Omega'\sigma'w';f = 0\rangle$ integrals analytically, using three parameters, namely, the effective nonrelativistic interaction potentials of the $A-I^+(^3\Pi)$, $A-I^+(^3\Sigma^-)$, and $A-I^-(^1\Sigma^+)$ fragments or V_Π, V_Σ, and V_-, as the functions of the distances ρ_α between the particle A and the iodine center $\alpha = a,b$. The list of formulas relevant for all first-tier IP states can be found in ref 9. For example, the matrix elements for the E−D pair of states are expressed as

$$V^{DIM}_{EE} = V^{DIM}_{DD} = \nu_a + \nu_b \quad V^{DIM}_{ED} = \nu_a - \nu_b$$
$$\nu_\alpha = \frac{1}{12}(5V^\alpha_\Pi + V^\alpha_\Sigma) - \frac{1}{4}(V^\alpha_\Pi - V^\alpha_\Sigma)\cos^2\beta_\alpha + \frac{1}{2}V^\alpha_- \quad (27)$$

where $V^\alpha_\Lambda = V_\Lambda(\rho_\alpha)$ and $V^\alpha_- = V_-(\rho_\alpha)$; $\Lambda = \Sigma, \Pi$, β_α is the angle between the r and ρ_α axes, $\alpha = a,b$.

Effective diatomic V_Π, V_Σ, and V_- potentials for $A = CF_4$ were obtained using the correlation relations proposed for the $Rg-I^\pm$ systems with Rg = He, Ne, and Ar.[40,41] The equilibrium properties (ρ_e and D_e) were estimated through the atomic radii and polarizabilities of the atoms and ions involved. The potentials were obtained by scaling the corresponding ab initio $Ar-I^\pm$ potentials[41]

$$V_\Lambda(\rho) = \frac{D_e^{CF_4}}{D_e^{Ar}}V^{Ar}_\Lambda\left(\frac{\rho_e^{Ar}\cdot\rho}{\rho_e^{CF_4}}\right) \quad (28)$$

where the upper indexes distinguish the parameters of the Ar−$I^\pm$ and $CF_4-I^\pm$ potentials.

The so-defined $CF_4-I^\pm$ effective potentials should be modified for use within the DIM PT1 model.[16,28,29] They contain the charge-induced dipole interactions, which are nonphysical for the whole CF_4-I_2 system. Therefore, the terms proportional to $-\alpha_A/\rho^4$ were eliminated from the diatomic potentials.

Full Interaction Matrix. The DIM PT1 and LR expressions for the interaction PESs and couplings are additive and provide the parametrization of the full interaction matrix (eq 9) that enters the EVCC-IOS scattering eq 8. To avoid spurious behavior of the interaction PESs at short range, where the R^{-6} dependence of the LR correction may overpower the DIM PT1 repulsion, the LR term was dumped by the function

$$g_d(R) = 1 - \sum_{k=1}^{6} \frac{(R/R_0)^{k-1}}{(k-1)!} \exp(-R/R_0) \qquad (29)$$

where $R_0 = 0.4$ Å guarantees the correct behavior of the PESs at $R \rightarrow 0$ and minor changes of interaction energies at R close to the equilibrium distance R_e.

The full interaction matrix takes the form

$$V_{n\nu'_n v_{i'}, n\nu_n v_i}(R,\theta) = \delta_{v_{i'}v_i}(\langle \nu'_n | V^{DIM}_{nn}(r,R,\theta) | \nu_n \rangle + g_d(R) \langle \nu'_n | V^{LR,2}_{nn}(r,R,\theta) | \nu_n \rangle) \qquad (30)$$

$$V_{n'\nu_{n'} v_{i'}, n\nu_n v_i}(R,\theta) = \delta_{v_{i'}v_i} \langle \nu_{n'} | V^{DIM}_{nn'}(r,R,\theta) | \nu_n \rangle + \xi_{v_{i'}v_i} \langle \nu_{n'} | V^{LR,1}_{nn',v_{i'}v_i}(r,R,\theta) | \nu_n \rangle \qquad (31)$$

if n, n' correspond to the dipole-coupled IP states of $E-D$, $\beta-\gamma$, and $D'-\delta$ and

$$V_{n'\nu_{n'} n_{i'}, n\nu_n \nu_i}(R,\theta) = \delta_{v_{i'}v_i} \langle \nu_{n'} | V^{DIM}_{nn'}(r,R,\theta) | \nu_n \rangle \qquad (32)$$

otherwise. Note that $i,i' = 0$, 3, 4 and $\xi_{v_0 v_3} = \xi_{v_0 v_4} = 1$, whereas $\xi_{v_3 v_4} = 0$.

4. Computational Details. All calculations were performed at the fixed collision energy $E_0 = 300$ cm^{-1}, and the rate constants were obtained using the hard-sphere approximation

$$k_{n'\nu_{n'} v_{i'}, n\nu_n v_i}(T) = \left(\frac{8kT}{\pi\mu}\right)^{1/2} \sigma_{n'\nu_{n'} v_{i'}, n\nu_n v_i}(E_0) \qquad (33)$$

where the temperature T roughly corresponds to 300 K. This approximation was found to be reasonable for $I_2(E)$ + Rg collisions.[9−11]

Two choices of the rovibronic channel basis were used. In the first one, hereafter the CC(18) model, vibrationally excited levels of the CF_4 were combined with all electronic states of the I_2 molecule; in the second, CC(6), CF_4 excitation was only allowed in the E and D electronic channels. In both cases and for all initial vibrational excitations v_E, the number of I_2 vibrational levels considered in each electronic channel was chosen to provide all partial cross sections converged to within 10%.

The vibrational problem for the I_2 molecule for each IP state was solved using the Numerov method and a set of spectroscopic potentials described in ref 9. The resulting wave functions were converted to Gauss−Legendre quadrature to calculate the integrals in eqs 30−32. The system of the EVCC-IOS eq 8 was solved by the modified log-derivative algorithm of Manolopoulos[42] on the grid of 2000 sectors from $R = 2$ to 30 Å. Twenty Gauss-Legendre nodes from 0 to $\pi/2$ were found to be sufficient to represent the IOS S matrix elements as functions of the θ angle (eq 11). Up to 400 partial waves in l were included to compute the cross sections by eq 12 or 13. The calculations were performed at each 10th partial wave, and the result was multiplied by 10. We verified that this procedure gives accurate results.

III. Results

CINATs between the IP states of the I_2 molecule in collisions with the CF_4 partner were investigated using the OODR spectroscopy by two groups. Pravilov and co-workers[7,8] examined the $E \rightarrow D$ channel for a wide range of initial vibrational excitations $v_E = 8-30$. For brevity, we will refer to these data as the high-v results. The low-v data for $v_E = 0-2$ have been recently reported by Stephenson and co-workers.[18] In addition to the $E \rightarrow D$ CINAT, these authors analyzed transitions to the β and D' states. These experiments gave the partial CINAT rate constants

TABLE 1: Total Room-Temperature Experimental and Theoretical Vibrationally Summed CINAT Rate Constants (in cm^3/s)[a]

		model		
v_E	final state	CC(6)	CC(18)	experiment[18]
0	D	6.5(−11)	7.9(−11)	1.1 ± 0.1(−10)
	D'	9.5(−11)	3.8(−10)	2.3 ± 0.2(−10)
	β	4.5(−11)	7.4(−11)	2.7 ± 0.2(−10)
	γ	7.3(−13)	8.5(−13)	
2	D	1.2(−10)	1.4(−10)	1.4 ± 0.1(−10)
	D'	4.3(−11)	2.8(−10)	2.5 ± 0.2(−10)
	β	2.4(−11)	1.2(−10)	3.1 ± 0.2(−10)
	γ	1.3(−11)	4.0(−12)	
	δ	4.9(−12)	1.1(−11)	

[a] The values in the parentheses designate the power of ten.

$$k_{n'}(\nu_E) = \sum_{\nu_{n'}} \sum_{v_{i'}} k_{n'\nu_{n'} v_{i'}, E\nu_E v_0} \qquad (34)$$

and VPDs resolved in the $I_2(n')$ vibrational state

$$P_{n'}(\nu_E, \nu_{n'}) = \sum_{v_{i'}} k_{n'\nu_n v_{i'}, E\nu_E v_0} / k_{n'}(\nu_E) \qquad (35)$$

The majority of the measurements were performed with rotationally excited $I_2(E, \nu_E, j = 55)$ molecules. We used the same value of j in our calculations.

1. Low-ν Results. The CINAT at $\nu_E \leq 2$ occurs at relatively low product state density and can be studied at the most sophisticated level. It provides an opportunity for quantitative assessment of the present model.

Partial CINAT rate constants are presented in Table 1. The level of agreement achieved for the CC(18) model is surprisingly good, taking into account a variety of approximations involved. Theory qualitatively reproduces the similarity in the population of the lowest IP states D', β, and D, though it gives the preference to the D' rather than to the β channel. Theory also predicts that the efficiency of the CINAT to higher γ and δ states increases with ν_E, but no analysis of the corresponding fluorescence was made in ref 18. Noteworthy, the inclusion of the vibrationally excited CF_4 states in all electronic channels is essential for correct determination of the CINAT branching ratios.

Vibrational product state distributions $P_{n'}(\nu_E, \nu_{n'})$ for the D', β, and D states are shown in Figures 1 and 2. The results of CC(6) and CC(18) calculations are presented together with experimental data and Franck−Condon (FC) factors. The vertical dotted line marks the energy of the initial level, while the solid line indicates the energy of the v_4 excitation of CF_4 relative to the initial energy.

It is evident that at $\nu_E = 0$, the v_4 mode of the partner can be excited through the near-resonant E−V mechanism only in the D' CINAT channel, while at $\nu_E = 2$, it can be excited in the β and D' channels. In other cases, as well as always for the v_3 mode, more or less substantial translational energy transfer is required to excite the partner. Decomposition of the computed partial rate constants shows that the contribution of the E−V transfer amounts to 55−80% of the total CINAT efficiency, whereas the contribution of the transitions assisted by translational energy is significantly lower.

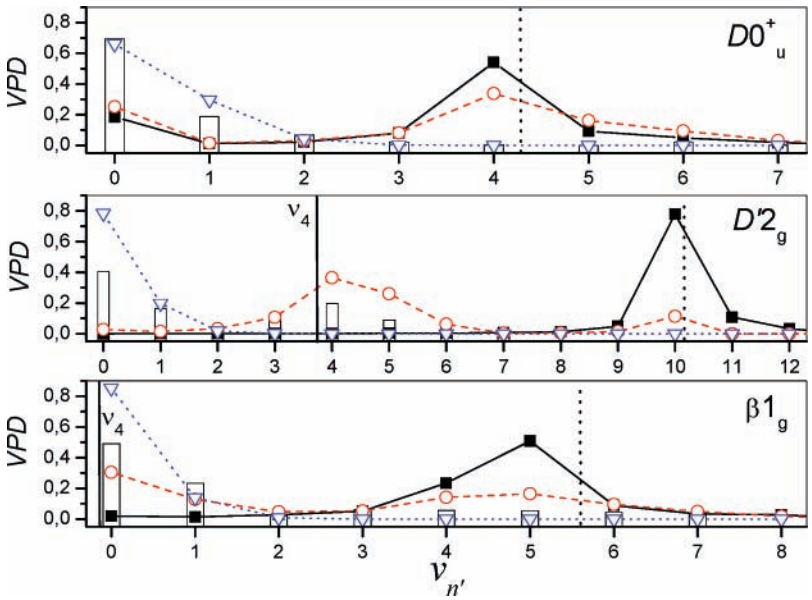

Figure 1. Measured and calculated vibrational product state distributions and Franck−Condon factors of the $I_2(E) + CF_4$ collisions in the final states D, D', and β at $v_E = 0$. Bars represent the experimental results, and squares and circles represent the calculations with the CC(6) and CC(18) models, respectively; the triangles are the FC factors. Vertical dotted lines indicate the positions of initial levels, and solid lines indicate excitation energies of the CF_4 vibrational modes.

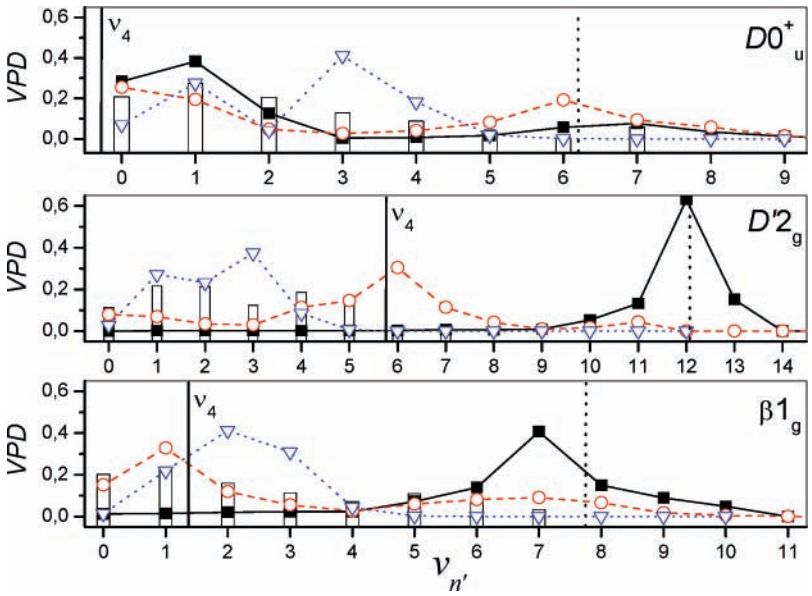

Figure 2. Same as Figure 1 but for $v_E = 2$.

Both measurements and calculations show that the branching ratios for transitions to the D', β, and D states in collisions with CF_4 are not far from those in collisions with Ar.[11−13] However, according to experiment, overall CINAT efficiency for CF_4 is higher by an order of magnitude. The CC(18) model gives a factor of 15 for the total rate constants and 5 for the transitions without E−V energy transfer. Thus, the enhancement with respect to Ar can be attributed both to longer range character of the CF_4−I_2 interaction due to larger effective size and polarizability of the partner and to additional contribution of the E−V processes in the CF_4 collisions.

Figures 1 and 2 shows that agreement between experimental and theoretical VPDs is not as good as that for the total rate constants. The actual shape of VPDs can be understood as a result of a compromise between the FC principle, which tends to maximize the population of the final states whose wave functions have maximum overlap with the initial one, and the energy gap law, which gives the preference to the near-resonant transitions with the minimum translational energy gain or release. The measured $E \rightarrow D$ distributions exhibit clear signatures of the FC trend,[18] while the calculated ones follow the energy gap law that manifests itself in the near-resonant maxima. By contrast, for the $I_2 + Ar$ collisions, both experiment and theory give broad $E \rightarrow D$ VPDs that do not show a prevalence of any trend. Stephenson and co-workers[18] argued that the internal degrees of freedom of CF_4, both rotational and vibrational, should increase the role of FC factors acting as a reservoir for translational energy. In addition, they have provided evidence for the excitation of the low-frequency v_2 vibrational mode of the CF_4 partner at 435 cm^{-1}. Neither rotations nor the v_2 vibration uncoupled from the ground state under the dipole approximation are included in the present model. Although indirectly, the near-resonant character of the calculated VPDs,

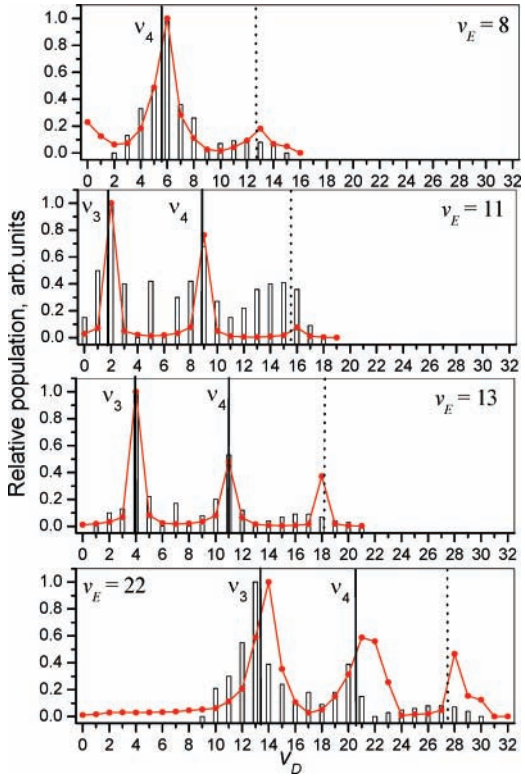

Figure 3. Experimental and calculated [model CC(6)] vibrational product state distributions (normalized to unity at the maximum) for E, $v_E \rightarrow D$, v_D transitions in collisions with CF_4 at $v_E = 8$, 11, 13, and 22. Vertical dotted lines mark the positions of the initial state, and the solid lines mark the excitation energies of the v_3 and v_4 modes with respect to the initial state.

together with the previous experience with Ar,[11] supports the conclusions of ref 18.

The CC(6) and CC(18) models agree with each other for the $E \rightarrow D$ but not for the $E \rightarrow D'$ and $E \rightarrow \beta$ CINATs. In the former model, the levels close to the resonance with the ground-state partner (dotted vertical marks in Figures 1 and 2) always dominate, while the latter model reduces their population in favor of the states close to the v_4 excitation. This is in much better agreement with experimental results, indicating that CF_4 vibrations can be excited even in the absence of the direct dipole−dipole interaction with the initial level, presumably through the asymptotically closed $I_2(D)$ + $CF_4(v_4)$ channels. This is in line with the previous finding that in collisions with rare gases, the D' and β states are populated indirectly through the intermediate D state.[9,25]

2. High-v Results. The product state density rapidly increases with the initial excitation v_E. The number of channels to be included in the CC(18) model becomes very large; therefore, we resorted to the simpler CC(6) approach that correctly describes the $E \rightarrow D$ CINAT channel, the only one for which quantitative experimental information is available at $v_E \geq 8$.[7,8]

We start the discussion with the vibrational product state distributions. Figure 3 compares the measured and calculated $P_D(v_E,v_D)$ (normalized to the highest population) for selected initial excitations. All distributions exhibit sharp maxima associated with v_4 and v_3 excitations of the partner (except the $v_E = 8$ case, where v_3 excitation requires large transfer of the translational energy). Theory reproduces these peaks very well (remarkable deviations are evident only at the highest $v_E = 22$ excitation considered).

In Figure 4, the calculated VPD for $v_E = 13$ is decomposed into the contributions related to the vibrational excitation of the

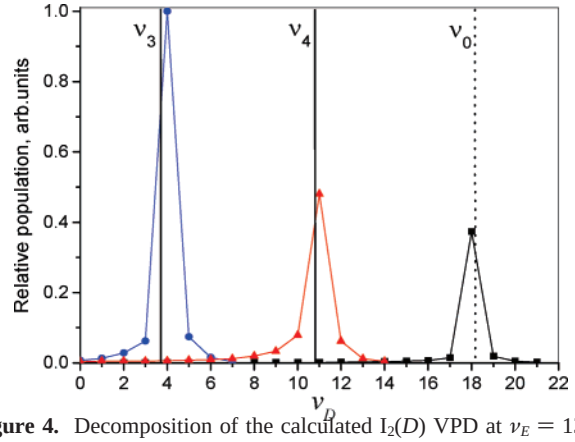

Figure 4. Decomposition of the calculated $I_2(D)$ VPD at $v_E = 13$ in terms of the transitions to different vibrational levels of the partner. Vertical lines mark the corresponding resonance energies.

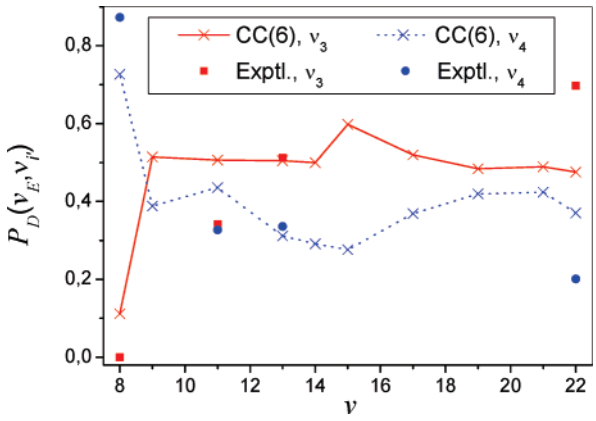

Figure 5. Populations of the v_3 and v_4 vibrational levels of the CF_4 fragment after the collisions with the $I_2(E, v_E)$ molecule.

partner. The overlap between them in v_D is negligibly small; therefore, each feature can be reliably assigned to a certain final state of the partner. It can be stated that $I_2(D)$ VPDs are also resolved in the vibrational states of the partner; probing one product, it is possible to obtain the vibrational distributions for both. The distributions for the CF_4 product defined as

$$P_D(v_E,v_{i'}) = \sum_{v_D} k_{Dv_Dv_{i'},Ev_Ev_0}/k_D(v_E) \qquad (36)$$

is easy to obtain from the calculated rate constants. For experimental distributions, $v_{i'}$ specifies the range of v_D in the summation (eq 36). As the summation boundaries, we chose the maxima (tentatively assigned to the $v_2 + v_4$ CF_4 excitation not included in our model[7]) between the v_3 and v_4 features and minima between the v_4 and v_0 features; see Figure 3. The populations of the boundary level were equally divided between the adjacent $v_{i'}$ populations. These distributions are depicted in Figure 5. Good agreement between experiment and theory is indicative of the possibility of quantitative decomposition of the $I_2(D)$ distributions into the distributions of the partner.

It is remarkable that theory and experiment agree with each other in assigning 80−95% of the total $E \rightarrow D$ CINAT probability to the transitions accompanied by v_3 and v_4 excitations of the partner. The average ratio of the E−V energy transfer efficiency to v_3 and v_4 levels is around 1.4, much smaller value than the squared ratio of the corresponding transition dipole moments (ca. 50). The difference in dipole excitation probabilities is compensated by the higher frequency of the v_3 mode that requires the transfer of seven extra I_2 vibrational quanta.

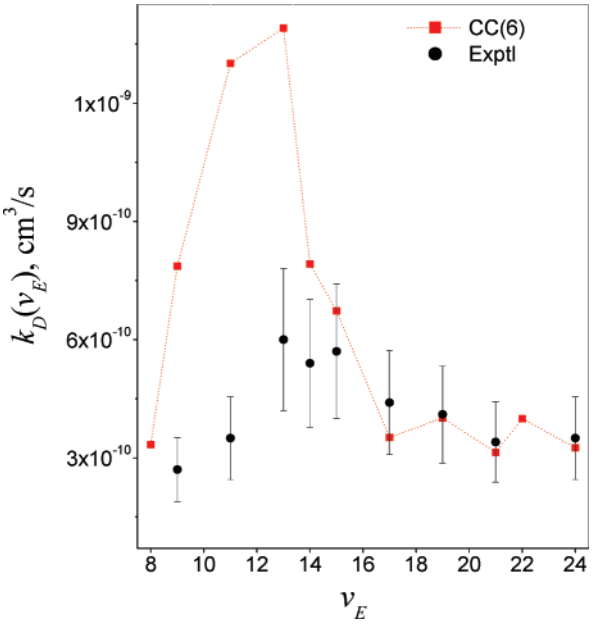

Figure 6. Room-temperature vibrationally summed $E \rightarrow D$ CINAT rate constant as a function of initial vibrational excitation. Error bars correspond to 30% accuracy, as indicated in ref 7.

Agreement between theory and experiment is worse for the transitions that leave a CF_4 fragment in the ground state (the maxima nearby the dotted vertical marks). The former gives sharp maxima; the latter gives broader bell-like features. This difference is in line with the results for the low-v case and can be viewed as proof that exaggerated propensity to the near-resonant transitions arises from the omission of the rotational degrees of freedom of the partner. Better agreement for the processes accompanied by the υ_3 and υ_4 excitations results from much a weaker influence of the rotations, which is suppressed by the $\Delta J = \pm 1$ selection rule for the dipole-induced transitions.

The total $E \rightarrow D$ CINAT rate constant is presented in Figure 6. Though the theory tends to overestimate it up to a factor of 5, a remarkable feature is the maximum at $v_E = 11-13$, where the near-resonant levels with very small energy gaps exist for both υ_4 and υ_3 channels. It mimics well the maximum of the measured rate constant around $v_E = 13$. Theory and experiment agree that at $v_E = 19$, the total efficiency of the $E \rightarrow D$ CINAT on CF_4 is six times higher than that on Ar.[14] However, a partial rate constant of CINATs without the CF_4 excitation is almost two times lower than the total rate constant for Ar, in contrast to the low-v results.

IV. Summary and Conclusions

We formulated an approximate theoretical model for the $I_2(E) + CF_4$ nonadiabatic collisions. The model treats the CF_4 partner as a spherical particle with an internal vibrational structure and accounts for the nonadiabatic transitions accompanied by the vibrational excitations of CF_4. We have constructed the relevant potential energy surfaces and coupling matrix elements using the diatomics-in-molecule perturbation theory corrected to the long-range interaction. The latter is treated using a special form of the intermolecular perturbation theory. It allows calculation of the first-order correction to the diabatic couplings due to the interaction of electronic (I_2) and vibrational (CF_4) transition dipole moments and the second-order induction-like correction to the interaction energy.

Within this model, the dynamics of the $I_2(E) + CF_4$ CINAT was investigated quantum mechanically for a wide range of initial vibrational excitations of the iodine molecule. The theory provides a good agreement with available experimental results for the vibrationally averaged CINAT rate constants and reasonably reproduces the vibrational product state distributions. The long-range coupling between the transition dipole moments of the colliding molecules strongly influences the CINAT dynamics. It induces the nonadiabatic transitions accompanied by the dipole-allowed excitations of the partner. Proceeding through direct near-resonant E−V energy transfer, these transitions may contribute more than 80% to the overall CINAT probability. In contrast, translational energy transfer is inefficient for the partner's excitation. These findings are in line with the simple semiclassical analysis by Pravilov and co-workers.[7]

The resonant character of the partner's excitation and the large mismatch in the vibrational frequencies in I_2 and CF_4 make it possible to determine the vibrational product state distributions for both particles from the single known I_2 VPD. This allows isolation of the contribution of the E−V energy transfer without probing the final states of the partner.

We suggest that the proposed theoretical model would be useful for studying a broad range of inelastic collision processes involving the spherical top molecules as the partners (providing that the corresponding PESs and couplings are known, especially at long range). Here, we considered one of the most complicated cases, electronic energy transfer in a diatomic molecule. It can be easily reduced to the nonadiabatic collisions of atoms or vibrationally inelastic processes in the diatoms. Present experience allows one to expect at least qualitatively correct results. However, our analysis indicates that the rotations of the ST partner can play a significant role. Though at present we see no way to take them into account without the great complications of the scattering problem, well-known statistical approximations or scaling laws could be attempted in seeking improvement.

Acknowledgment. We thank Dr. T. V. Tscherbul, Professor A. M. Pravilov, and Professor T. A. Stephenson for instructive comments and sharing their results. Support from the Russian Basic Research Fund (Project No.'s 05-03-32371 and 05-07-90067), and the Russian Science Support Foundation is gratefully acknowledged.

References and Notes

(1) Ellenbroek, T.; Toennies, P. J. *Chem. Phys.* **1982**, *71*, 309.

(2) Hansel, A.; Oberhofer, N.; Lindinger, W.; Zenevich, V. A.; Billing, G. D. *Int. J. Mass Spectrom.* **1999**, *185*−*187*, 559.

(3) Yamasaki, K.; Fujii, H.; Watanabe, S.; Hatano, T.; Tokue, I. *Phys. Chem. Chem. Phys.* **2006**, *8*, 1936.

(4) Thomas, J. M.; Jeffries, J. B.; Kaufman, F. *Chem. Phys. Lett.* **1983**, *102*, 50.

(5) Ellenbroek, T.; Giertz, U.; Noll, M.; Toennies, J. P. *J. Phys. Chem.* **1982**, *86*, 1153.

(6) Alekseev, V.; Setser, D. W. *J. Phys. Chem.* **1996**, *100*, 5766.

(7) Akopyan, M. E.; Pravilov, A. M.; Stepanov, M. B.; Zakharova, A. A. *Chem. Phys.* **2003**, *287*, 399.

(8) Akopyan, M. E.; Bibinov, N. K.; Kokh, D. B.; Pravilov, A. M.; Sharova, O. L.; Stepanov, M. B. *Chem. Phys.* **2001**, *263*, 459.

(9) Tscherbul, T. V.; Buchachenko, A. A.; Akopyan, M. E.; Poretsky, S. A.; Pravilov, A. M.; Stephenson, T. A. *Phys. Chem. Chem. Phys.* **2004**, *6*, 3201.

(10) Akopyan, M. E.; Novikova, I. Yu.; Poretsky, S. A.; Pravilov, A. M.; Smolin, A. G.; Tscherbul, T. V.; Buchachenko, A. A. *J. Chem. Phys.* **2005**, *122*, 204318.

(11) Tscherbul, T. V.; Suleimanov, Yu. V.; Buchachenko, A. A. *Russ. J. Phys. Chem.* **2006**, *80*, 2196.

(12) Fecko, C. J.; Freedman, M. A.; Stephenson, T. A. *J. Chem. Phys.* **2002**, *116*, 1361.

(13) Chandra, P. P.; Stephenson, T. A. *J. Chem. Phys.* **2004**, *121*, 2985.

(14) Akopyan, M. E.; Buchachenko, A. A.; Lukashov, S. S.; Poretsky, S. A.; Pravilov, A. M.; Suleimanov, Yu. V.; Torgashkova, A. S.; Tscherbul, T. V. *Chem. Phys. Lett.* **2007**, *436*, 1−6.
(15) Suleimanov, Yu. V.; Tscherbul, T. V.; Buchachenko, A. A. *Russ. J. Phys. Chem.* **2007**, *81*, 63.
(16) Tscherbul, T. V.; Zaitsevskii, A. V.; Buchachenko, A. A.; Stepanov, N. F. *Russ. J. Phys. Chem.* **2003**, *77*, 511.
(17) Fecko, C. J.; Freedman, M. A.; Stephenson, T. A. *J. Chem. Phys.* **2001**, *115*, 4132.
(18) Hutchison, J. M.; Carlisle, B. R.; Stephenson, T. A. *J. Chem. Phys*. **2006**, *125*, 194313.
(19) Steinfeld, J. I. *J. Phys. Chem. Ref. Data* **1984**, *13*, 445.
(20) Brand, J. C. D.; Hoy, A. R. *Appl. Spectrosc. Rev.* **1987**, *23*, 285.
(21) Lawley, K. P.; Donovan, R. J. *J. Chem. Soc., Faraday Trans.* **1993**, *89*, 1885.
(22) Lawley, K. *Chem. Phys.* **1988**, *127*, 363.
(23) Sjödin, A. M.; Ridley, T.; Lawley, K. P.; Donovan, R. J. *J. Chem. Phys.* **2004**, *120*, 2740.
(24) Buchachenko, A. A.; Stepanov, N. F. *J. Chem. Phys.* **1996**, *104*, 9913.
(25) Tscherbul, T. V.; Buchachenko, A. A. *J. Phys. B* **2004**, *37*, 1605.
(26) Kouri, D. J. In *Atom−Molecule Collision Theory*; Bernstein, R. B., Ed.; Plenum: New York, 1979; p 301.
(27) Parker, G. A.; Pack, R. T. *J. Chem. Phys.* **1978**, *68*, 1585.
(28) Last, I.; George, T. F. *J. Chem. Phys.* **1987**, *87*, 1183.
(29) Last, I.; George, T. F. *J. Chem. Phys.* **1988**, *89*, 3071.
(30) Grigorenko, B. L.; Nemukhin, A. V.; Apkarian, V. A. *J. Chem. Phys.* **1996**, *104*, 5510.
(31) Nemukhin, A. V.; Grigorenko, B. L.; Skasyrskaya, E. Ya.; Topol, I. A.; Burt, S. K. *J. Chem. Phys.* **2000**, *112*, 513.
(32) Ovchinnikov, M.; Apkarian, V. A. *J. Chem. Phys.* **1999**, *110*, 9842.
(33) Gray, C. G. *Can. J. Phys.* **1968**, *46*, 135.
(34) Jaannotte, A. C.; Legler, D.; Overend, J. *Spectrochim. Acta, Part A* **1973**, *29*, 1915.
(35) Elliot, D. S.; Ward, J. F. *Mol. Phys.* **1984**, *51*, 45.
(36) Holtermann, D. L.; Lee, E. K. C.; Nanes, R. *J. Chem. Phys.* **1982**, *77*, 5327.
(37) Durant, J. L.; Kaufman, F. *Chem. Phys. Lett.* **1987**, *142*, 246.
(38) Zare, R. N. *Angular Momentum*; Wiley: New York, 1988.
(39) Maroulis, G. *Chem. Phys. Lett.* **1996**, *259*, 654.
(40) Cappelletti, D.; Liuti, G.; Pirani, F. *Chem. Phys. Lett.* **1991**, *183*, 297.
(41) Buchachenko, A. A.; Tscherbul, T. V.; Kłos, J.; Szczęśniak, M. M.; Chałasiński, G.; Webb, R.; Viehland, L. A. *J. Chem. Phys.* **2005**, *122*, 194311.
(42) Manolopoulos, D. E. *J. Chem. Phys.* **1986**, *85*, 6425.